AGU PUBLICATIONS

JGR

Journal of Geophysical Research: Space Physics

RESEARCH ARTICLE
10.1002/2016JA023175

Special Section:
Geospace system responses to the St. Patrick's Day storms in 2013 and 2015

Timescale separation in the solar wind-magnetosphere coupling during St. Patrick's Day storms in 2013 and 2015

T. Alberti[1], G. Consolini[2], F. Lepreti[1], M. Laurenza[2], A. Vecchio[3], and V. Carbone[1]

[1]Department of Physics, University of Calabria, Rende, Italy, [2]INAF-Istituto di Astrofisica e Planetologia Spaziali, Rome, Italy, [3]LESIA-Observatoire de Paris, Meudon, France

Key Points:
- Novel analysis approaches clearly indicate the existence of a relevant timescale separation in the solar wind-magnetosphere coupling
- Short-timescales (200 min) fluctuations, triggered by changes of the interplanetary conditions, are mainly related to internal processes
- The magnetospheric dynamics at timescales longer than 200 min resembles the changes observed in the solar wind/IMF features

Correspondence to:
T. Alberti,
tommaso.alberti@unical.it

Citation:
Alberti, T., G. Consolini, F. Lepreti, M. Laurenza, A. Vecchio, and V. Carbone (2017), Timescale separation in the solar wind-magnetosphere coupling during St. Patrick's Day storms in 2013 and 2015, *J. Geophys. Res. Space Physics*, *122*, 4266–4283, doi:10.1002/2016JA023175.

Received 15 JUL 2016
Accepted 15 MAR 2017
Accepted article online 21 MAR 2017
Published online 19 APR 2017

Abstract In this work, we present a case study of the relevant timescales responsible for coupling between the changes of the solar wind and interplanetary magnetic field (IMF) conditions and the magnetospheric dynamics during the St. Patrick's Day Geomagnetic Storms in 2013 and 2015. We investigate the behavior of the interplanetary magnetic field (IMF) component B_z, the Perreault-Akasofu coupling function and the *AE*, *AL*, *AU*, *SYM-H*, and *ASY-H* geomagnetic indices at different timescales by using the empirical mode decomposition (EMD) method and the delayed mutual information (DMI). The EMD, indeed, allows to extract the intrinsic oscillations (modes) present into the different data sets, while the DMI, which provides a measure of the total amount of the linear and nonlinear shared information (correlation degree), allows to investigate the relevance of the different timescales in the solar wind-magnetosphere coupling. The results clearly indicate the existence of a relevant timescale separation in the solar wind-magnetosphere coupling. Indeed, while fluctuations at long timescales ($\tau > 200$ min) show a large degree of correlation between solar wind parameters and magnetospheric dynamics proxies, at short timescales ($\tau < 200$ min) this direct link is missing. This result suggests that fluctuations at timescales lower than 200 min, although triggered by changes of the interplanetary conditions, are mainly dominated by internal processes and are not directly driven by solar wind/IMF. Conversely, the magnetospheric dynamics in response to the solar wind/IMF driver at timescales longer than 200 min resembles the changes observed in the solar wind/IMF features. Finally, these results can be useful for Space Weather forecasting.

1. Introduction

The Earth's magnetospheric dynamics in response to changes of the solar wind (SW) and interplanetary magnetic field (IMF) conditions during magnetic storms and substorms is the result of both externally driven and internal processes that can be investigated via a set of geomagnetic indices. These geomagnetic indices monitor the changes of some of the most important current systems. In particular, the variations of the auroral electrojet indices (*AE*, *AU*, *AL*, and *AO*) and the low-latitude geomagnetic ones (*Dst*, *SYM-H*, and *ASY-H*) are associated with the changes of the high-latitude ionospheric auroral electrojets and the equatorial ring current during geomagnetic substorms and storms, respectively. The changes of these current systems result from the magnetospheric configuration and dynamics, being affected by the energy transfer from the solar wind to different regions of the magnetosphere through electromagnetic processes [*Perreault and Akasofu*, 1978]. This interaction involves a considerable energy transfer by the solar wind, which manifests itself in several fast phenomena occurring in the magnetosphere such as auroral displays, magnetic substorms, and storms [*Tsurutani et al.*, 2015].

As a consequence of the solar wind-magnetosphere interaction, these indices display both regular and irregular variations/fluctuations on a very wide interval of timescales [*Merrill et al.*, 1996; *De Michelis et al.*, 2015], ranging from a few tens of minutes up 200 min. The observed multiscale variations/fluctuations have been shown to be also due to a complex and nonlinear dynamics of the Earth's magnetosphere [*Tsurutani et al.*, 1990; *Sharma*, 1995; *Vassiliadis*, 2006; *Consolini and De Michelis*, 2014]. Indeed, in the last two decades many studies evidenced how the multiscale character of the fluctuations/variations of geomagnetic indices is associated with fractal/multifractal scaling features of the corresponding time series [*Consolini et al.*, 1996; *Consolini*, 1997; *Uritsky and Pudovkin*, 1998; *Kovacs et al.*, 2001; *Wanliss*, 2005; *Consolini and De Michelis*, 2011] and power law distributions of the associated energy dissipation events [*Consolini*, 1997, 2002; *Wanliss and Uritsky*, 2010].

All these features have been interpreted as evidences of a far-from-equilibrium nonlinear dynamics near a critical state [see, e.g., *Klimas et al.*, 1996; *Sitnov et al.*, 2001; *Consolini and Chang*, 2001; *Consolini*, 2002; *Uritsky et al.*, 2002; *Consolini et al.*, 2008]. An important consequence of this nonlinear and near-critical-state dynamics of the Earth's magnetosphere is that there is not a one-to-one correspondence between the SW/IMF condition changes and those of the magnetospheric current systems as monitored by geomagnetic indices [*Sitnov et al.*, 2001; *Consolini*, 2002]. In other words, the dynamics of the magnetospheric currents and of the overall magnetosphere, although triggered by the variation of the interplanetary conditions, is strongly affected by the internal conditions. This is exactly what has been understood since the early works on the nonlinear and pseudochaotic dynamics of the Earth's magnetosphere [see, e.g., *Tsurutani et al.*, 1990; *Klimas et al.*, 1996].

A relevant issue in the study of the solar wind-magnetosphere coupling is related to the different timescales involved in the internal and externally driven processes. For instance, geomagnetic substorms are mainly the result of two different phenomena: the increase of plasma convection and fast energy relaxations occurring in the near-Earth tail central plasma sheet (CPS) [*Rostoker et al.*, 1987; *Kamide and Kokubun*, 1996; *Consolini and De Michelis*, 2005]. These two phenomena, which are connected to the direct-driven and loading-unloading processes, are characterized by different timescales. In particular, while loading-unloading processes generally occur on short timescale ($\tau < 100$ min) and manifest themselves in terms of coherent intermittent activity bursts, the externally direct-driven ones take place on longer timescales [*Kamide and Kokubun*, 1996; *Consolini and De Michelis*, 2005].

The identification of the timescales directly connected to the external solar wind variability and to the internal magnetospheric dynamics is also a relevant issue in the framework of Space Weather studies. Indeed, this information is of fundamental importance to know to what extent we can forecast the magnetospheric dynamics starting from the measurement of the solar wind conditions. Attempts to forecast high-latitude geomagnetic disturbances as monitored by auroral electrojet indices (such as, *AE* index) via artificial neural networks have clearly shown how *AE* variations on timescales shorter than 1 h, cannot be correctly forecasted from IMF and solar wind plasma parameters only [see, e.g., *Pallocchia et al.*, 2007]. These studies suggest that fluctuations on timescale shorter than 1 h are essentially not coupled to solar wind variations but result from internal magnetospheric processes only.

In this work, we present a detailed study of the timescale coupling between SW/IMF condition changes, and the magnetospheric response in the course of the two St. Patrick's Day geomagnetic storms occurred in 2013 and 2015. To investigate the range of the coupled timescales, we use the empirical mode decomposition (EMD), which is particularly suitable for the analysis of nonlinear and nonstationary time series [*Huang et al.*, 1998], and the delayed mutual information (DMI), which is capable of providing a measure of the total linear and nonlinear correlation in terms of shared information.

2. Data and Methods

2.1. Data Sets and Geospace Conditions

We focus our analysis of relevant timescales involved into the solar wind-magnetosphere coupling considering two periods of 21 days from 10 to 30 of March 2013 and March 2015. These time intervals, which refer to the maximum phase (2013) of the Solar Cycle no. 24 (maximum sunspot number was observed in April 2014) and to the descending (2015) one, comprise both periods of low geomagnetic activity and the famous St. Patrick's Day geomagnetic storms. In particular, during the considered period in 2013, a halo coronal mass ejection (CME) was emitted on 15 March at 07:12, associated with an M1-flare located at N11E12 in the Active Region (AR) NOAA 1692. The CME had a linear speed of 1063 km/s and hit the Earth's magnetosphere at 06:00 UT on 17 March 2013 (storm sudden commencement, SSC), with the speed of the solar wind jumping from about 400 km/s to 750 km/s. Moreover, the CME's magnetic field was quite strong and oriented southward. The impact produced first a compression of the Earth's magnetosphere (solar wind pressure P_{SW} rose of a factor ~10) and, consequently to the southward orientation of the IMF B_z component, sparked a moderately strong ($Kp = 6$) geomagnetic storm.

In the same day of 2015, an asymmetric partial halo CME was observed at 01:48, having a linear speed of 719 km/s, and it was associated with a long duration C9.1 flare (location S22W25 in AR NOAA 2297). A shock in the solar wind parameters was observed by the ACE satellite shortly after 04:00 UT on 17 March, the solar wind speed jumping from 400 km/s to slightly above 500 km/s, then gradually increasing to a maximum of nearly 700 km/s over the next few hours. Except for a brief interruption between 09:00 and 11:00 UT,

the vertical component of the interplanetary magnetic field was consistently southward at about −20 nT from around 05:00 UT till 23:00 UT. First, the CME impact compressed the Earth's magnetosphere consequently to an increase of the flow pressure of a factor ∼3 ($p_{SW} \sim 15-20$ nPa) and, later, due to a southward turning of the IMF B_z component occurred at ∼06:00 UT, a relatively mild G1-class ($Kp = 5$) geomagnetic storm started. Since then, however, the storm has intensified to G4-class ($Kp = 8$), ranking it as the strongest geomagnetic storm of the current solar cycle (see http://swpc.noaa.gov/).

In this study, we use solar wind time series obtained from Advanced Composition Explorer (ACE) spacecraft (http://cdaweb.gsfc.nasa.gov), located at the Lagrangian point L1. In particular, we use data related to the three components (B_x, B_y, and B_z) of the interplanetary magnetic field (IMF) in GSM coordinates and the solar wind plasma bulk speed. In this way, we construct the Perrault-Akasofu coupling function ϵ which is defined as [*Perreault and Akasofu*, 1978]

$$\epsilon = \frac{4\pi}{\mu_0} l_0^2 v B^2 \sin^4(\theta_c/2) \quad [\mathrm{GW}] \tag{1}$$

where $\mu_0 = 4\pi \times 10^{-7}$ N/A^2 is the permeability of free space, $l_0 = 7\ R_E$ is the stand-off distance of the nose of the magnetosphere (also known as "effective cross-sectional area," "dayside magnetopause scale length," or simply seen as an empirical determined scale factor [*Perreault and Akasofu*, 1978; *Kan and Lee*, 1979; *Akasofu*, 1983; *Finch and Lockwood*, 2007]), v is the solar wind speed (in km/s), B is the magnitude of the solar wind magnetic field (in nT), and θ_c is the clock angle defined as

$$\theta_c = \begin{cases} \tan^{-1}\left(\left|\frac{B_y}{B_z}\right|\right), & \text{if } B_z > 0 \\ \pi - \tan^{-1}\left(\left|\frac{By}{Bz}\right|\right), & \text{if } B_z < 0. \end{cases}$$

Moreover, we analyze geomagnetic time series of the low-latitude *SYM-H* and *ASY-H* indices and the auroral electrojet indices, *AE*, *AU*, and *AL*, retrieved at OMNI website (http://omniweb.gsfc.nasa.gov). All the considered geomagnetic time indices have a 1 min time resolution. The *SYM-H* (a 1 min version of the well-known *Dst* index) and *ASY-H* indices, being derived from a network of near-equatorial geomagnetic observatories, allows us to get an estimate of the ring current dynamics and of the asymmetric low-latitude disturbance (partial ring current), respectively, in the course of a storm [*Sugiura and Poros*, 1971; *Kawasaki and Akasofu*, 1971; *Crooker and Siscoe*, 1971; *Crooker*, 1972; *Clauer and McPherron*, 1980; *Clauer et al.*, 1983]. On the other hand, the auroral electroject (*AE*, *AU*, and *AL*) indices (with 1 min resolution), derived from variations of the horizontal component (H) of the geomagnetic field at selected observatories along the auroral zone in the Northern Hemisphere [*Davies and Sugiura*, 1966], provide an estimation of the intensity of the electrojet currents in the auroral ionosphere and of the energy deposition in those regions [*Ahn et al.*, 1983]. In particular, *AE* index represents the overall activity of the auroral electrojets, while the *AU* and *AL* indices quantify the current intensity variations of the eastward and westward auroral electrojets, which are mainly related to the tail activity during magnetic storms and substorms.

Figure 1 shows the time series of the considered quantities (*SYM-H*, IMF-B_z, ϵ, *ASY-H*, *AE*, *AU*, and *AL*) for the two selected periods relative to the 2013 and 2015 St. Patrick's Day storms.

2.2. The Empirical Mode Decomposition (EMD) Method

The standard approach to identify the relevant timescales in a time series is based on Fourier analysis. Although this method is powerful in the case of stationary signals, it can produce fake results when it is applied to nonstationary time series. An alternative method to unveil the characteristic timescales of nonstationary signals is the empirical mode decomposition (EMD) technique, introduced by *Huang et al.* [1998] [see also *Wu and Huang*, 2004], as a preconditioning method for the application of the Hilbert transform. EMD is an adaptive method based on the local characteristics of the data, useful to analyze natural signals [*Vecchio et al.*, 2010a, 2010b, 2012a; *Alberti et al.*, 2014; *Vecchio et al.*, 2017], also including geomagnetic time series [*De Michelis et al.*, 2012; *De Michelis and Consolini*, 2015]. Particularly, the EMD does not require to have any "a priori" assumption on the functional form of the basis of the decomposition. This allows us to carry out local nonstationary and nonlinear features from each time series which are usually far from the decomposition properties obtained with fixed eigenfunctions. Here we use the same approach as proposed by *Huang et al.* [1998], with similar stopping criterion (i.e., the Cauchy convergence test with $\sigma = 0.3$), as previously used in other works [*Alberti et al.*, 2014, 2016] in which more details about the EMD procedure can be found. In what follows we provide a brief description of the method.

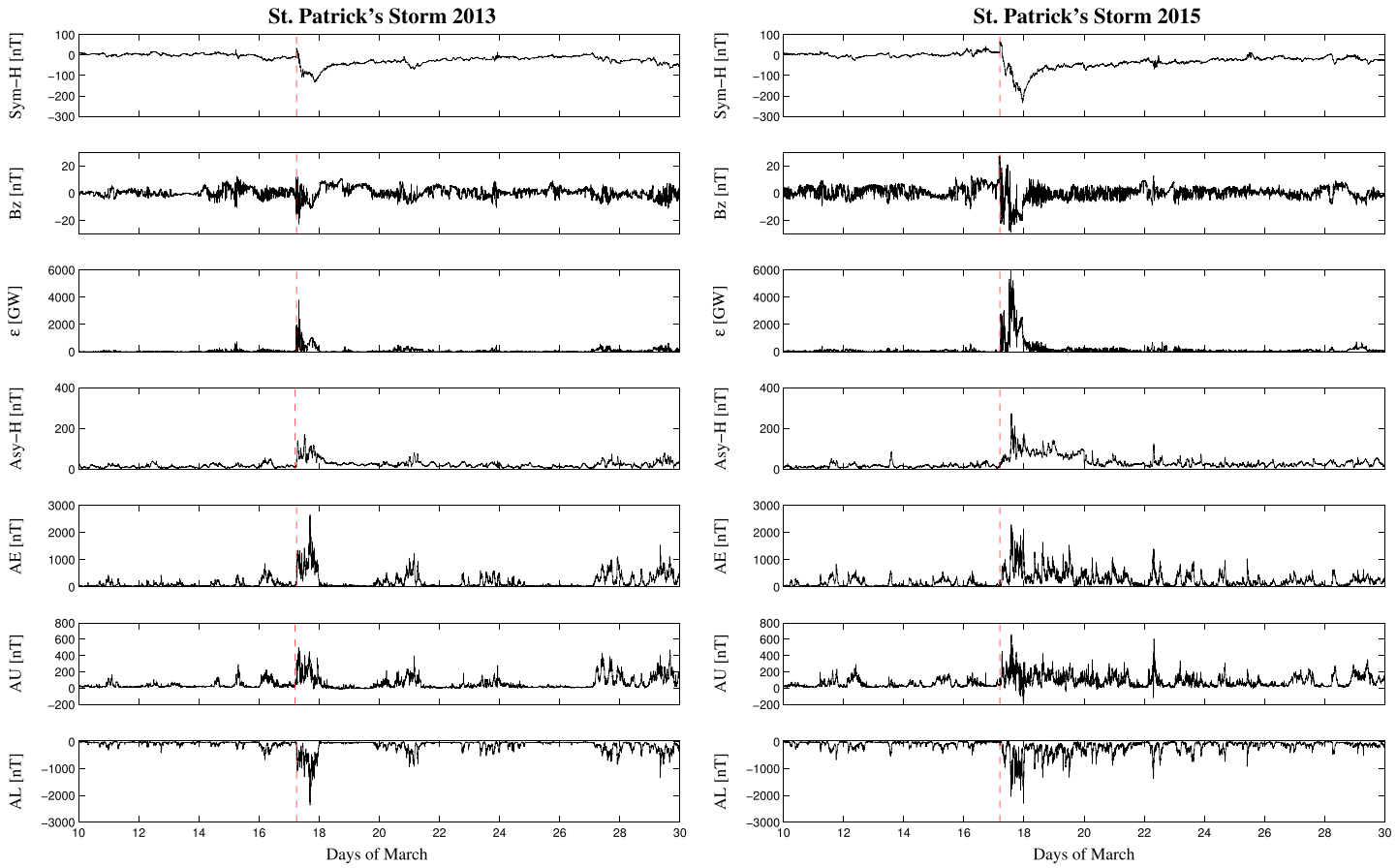

Figure 1. Time behavior of the solar wind parameters and the geomagnetic indices for both Storm time periods. The red dashed line identifies the SSC time.

A given time series $X(t)$ is decomposed into a set of N empirical modes $C_n(t)$, called intrinsic mode functions (IMFs) and ordered by increasing characteristic timescale, plus a residue $r(t)$. The decomposition reads

$$X(t) = \sum_{n=1}^{N} C_n(t) + r(t) \tag{2}$$

where each IMF is characterized by a time-dependent amplitude and phase ($C_n(t) = A_n(t)\sin(\phi_n(t))$, where $A_n(t)$ and $\phi_n(t)$ are the time-dependent amplitude and phase, respectively), and it is directly obtained from the time series with no a priori assumptions, regarding their nature, via an iterative procedure. Each IMF represents a local oscillatory component and the whole set of the IMFs becomes the basis of the decomposition (see *Huang et al.* [1998], *De Michelis et al.* [2012], and *Alberti et al.* [2014] for more details).

An example of the results of EMD analysis is shown in Figures 2 and 3 for the IMFs obtained using the *SYM-H* and *AE* indices for both periods. A set of $n = 15$ (14) and $n = 16$ (15) modes are extracted for the March 2013 (2015) time periods from *SYM-H* and *AE* indices, respectively, with characteristic timescales ranging from $\tau = 4$ min to $\tau \sim 10^4$ min. A similar number (14–17) of IMFs is found for the other parameters (B_z, ϵ, *ASY-H*, *AU*, and *AL*) in both selected time intervals.

To characterize the typical timescale associated with every IMFs, different methods can be used, from spectral method, based on the Fourier analysis of each IMFs, to autocorrelation-based methods and Max-Max/min-min distance once. Here we use the spectral method. In particular, the characteristic mean frequency f_n of all the IMFs is estimated by means of the associated Fourier power spectral density $S_n(f)$ as

$$f_n = \frac{\int_0^\infty f S_n(f)\mathrm{d}f}{\int_0^\infty S_n(f)\mathrm{d}f} \tag{3}$$